

# Amorphous Conjugated Carbazole Trimers for Photorefractive Materials

Yadong Zhang,<sup>†</sup> Tatuso Wada,<sup>\*,†,‡</sup> Liming Wang,<sup>‡</sup> and Hiroyuki Sasabe<sup>†,‡</sup>

Core Research for Evolutional Science and Technology (CREST), JST, and Frontier Research Program, The Institute of Physical and Chemical Research (RIKEN), Hirosawa 2-1, Wako, Saitama 351-01, Japan

Received March 3, 1997. Revised Manuscript Received July 9, 1997<sup>⊗</sup>

New conjugated carbazole trimers for photorefractive materials have been synthesized by Pd-catalytic coupling reaction. These trimers were demonstrated to be amorphous by both differential scanning calorimeter and X-ray diffraction. In these carbazole trimers, three carbazole rings are  $\pi$ -conjugated through ethynyl group and act as a charge transporting agent. Peripheral carbazoles substituted with acceptor groups can be served as an electrooptic chromophore. The photoconductivity, electrooptic effect, and photorefractive properties of the conjugated carbazole trimer substituted with dicyanovinyl group doped with 2,4,7-trinitro-9-fluorenone as a sensitizer are reported.

## Introduction

Photorefractive materials have numerous potential applications, including high-density optical data storage, optical image processing, phase conjugated mirrors, dynamic holography, optical computing, parallel optical logic, and pattern recognition, etc.<sup>1</sup> The photorefractive effects in a variety of inorganic electrooptic (EO) crystals have been extensively studied, and many different devices based on inorganic photorefractive crystals have also been proposed and developed.<sup>2–4</sup> The first organic photorefractive crystal and polymeric photorefractive material were reported in 1990 and 1991, respectively.<sup>5,6</sup> Since these reports, considerable progress has been made in the research on the optimization of organic photorefractive materials.<sup>7–9</sup> Amorphous photorefractive materials offer many advantages over the photorefractive crystals, such as large optical nonlinearities, low dielectric constants, low cost, structural flexibility, and ease of fabrication.

To be photorefractive, a material should have the following processes: charge generation, charge transporting and trapping (photoconductive process), as well as an EO response. When light is incident on a photorefractive material, if the incident light is not uniform in intensity, photogenerated charges migrate

through the charge transporting component from the illuminated area to the dark area, where these charges get trapped. The resulting charge redistribution creates a space charge field which changes the refractive index via EO effects. According to the requirements and the mechanism of the photorefractive effects, photorefractive materials must be multifunctional materials. For amorphous organic photorefractive materials, this multifunctionality can be achieved by two design approaches: the guest–host composite approach<sup>7,8</sup> and the full-functional polymeric approach.<sup>9</sup> Most of the reported amorphous photorefractive materials are developed from guest–host composite system using a nonlinear optical polymer,<sup>6,10</sup> a charge transporting polymer,<sup>11–14</sup> or an inert polymer<sup>15</sup> as a host doped with other corresponding necessary functional components. Recently, bifunctional chromophores have been reported and they are served as a charge transporting agent as well as a second-order nonlinear optical component.<sup>16,17</sup> The composite materials approach has the advantage of ease of optimization for the functionality by independently varying the nature and concentration of each component. However, there are inherent problems of phase separation in these doped systems which limits the concentrations of active moieties. To overcome the problem of phase separation, fully functional polymers with all necessary functional groups either in the polymeric main chain or in the side chain have the evident advantage of long-term stability and minimized phase separation.<sup>9,18–20</sup> However, the time-consuming

\* To whom correspondence should be addressed.

<sup>†</sup> CREST.

<sup>‡</sup> Frontier Research Program.

<sup>⊗</sup> Abstract published in *Advance ACS Abstracts*, October 15, 1997.

(1) Günter, P.; Huignard, J.-P., Eds. *Photorefractive Materials and Their Applications*; Springer-Verlag: New York, 1988; Parts I, II, Topics in Applied Physics Vols. 61 and 62.

(2) Hesselink, L.; Kratzig, E.; Ringhofer, K. H. *J. Opt. Soc. Am. B* **1994**, *11*, 1648.

(3) Feinberg, J.; Fischer, B. *J. Opt. Soc. Am. B* **1992**, *9*, 1404.

(4) Roosen, G.; Huignard, J.-P.; Gronin-Golomb, M. *J. Opt. Soc. Am. B* **1990**, *7*, 2242.

(5) Sutter, K.; Hulliger, J.; Günter, P. *Solid State Commun.* **1990**, *74*, 867.

(6) Ducharme, S.; Scott, J. C.; R. J. Tweig, R. J.; Moerner, W. E. *Phys. Rev. Lett.* **1991**, *66*, 1846.

(7) Moerner, W. E.; Silence, S. M. *Chem. Rev.* **1994**, *94*, 127.

(8) Zhang, Y.; Burzynski, R.; Ghosal, S.; Casstevens, M. K. *Adv. Mater.* **1996**, *8*, 111.

(9) Yu, L.; Chan, W. K.; Peng, Z.; Gharavi, A. *Acc. Chem. Res.* **1996**, *29*, 13.

(10) Liphardt, M.; Goonesekera, A.; Jones, B. E.; Ducharme, S.; Takacs, J. M.; Zhang, L. *Science* **1994**, *263*, 367.

(11) Zhang, Y.; Cui, Y.; Prasad, P. N. *Phys. Rev. B* **1992**, *46*, 9900.

(12) Silence, S. M.; Walsh, C. A.; Scott, J. C.; Moerner, W. E. *Appl. Phys. Lett.* **1992**, *61*, 2967.

(13) Malliaras, G. G.; Krasnikov, V. V.; Bolink, H. J.; Hadziioannou, G. *Appl. Phys. Lett.* **1994**, *65*, 262.

(14) Zobel, O.; Eckl, M.; Strohhriegl, P.; Haarer, D. *Adv. Mater.* **1995**, *7*, 911.

(15) Yokoyama, K.; Arishima, K.; Shimada, T.; Sukegawa, K. *Jpn. J. Appl. Phys.* **1994**, *33*, 1029.

(16) Zhang, Y.; Ghosal, S.; Casstevens, M. K.; Burzynski, R. *Appl. Phys. Lett.* **1995**, *66*, 256.

(17) Silence, S. M.; Scott, J. C.; Stankus, J. J.; Moerner, W. E.; Moylan, C. R.; Bjorklund, G. C.; Tweig, R. J. *J. Phys. Chem.* **1995**, *99*, 4096.

chemical synthesis and difficulty in rational design are constant challenges. Polymers with both charge transporting and EO functions have also been developed for photorefractive materials.<sup>21,22</sup> These bifunctional polymers can overcome the problem in rational design and minimize phase separation. Photorefractive effects have been demonstrated in these types of systems and the high-efficient photorefractive effects were obtained from guest–host polymer composites.<sup>23,24</sup> Recently, glassy molecules with charge transporting and EO functions have been reported and demonstrated to show high performance of the photorefractive effects.<sup>25</sup>

It is well-known that carbazole compounds exhibit photoconductive properties and have internal donor group in the 9-position. After the various acceptor groups are introduced to 3- and 6-positions, carbazole compounds show both photoconductivity and second-order nonlinearity.<sup>26</sup> Carbazole monomers and polymers used as a photoconductive component and an EO chromophore have already been developed.<sup>23,27–29</sup> Our molecular design goal is development of amorphous multifunctional chromophores to overcome the problem of phase separation for photorefractive applications. To achieve our target, carbazole ring is used as a basic building block for the design approach to photorefractive materials. In the case of multicomponent photorefractive material systems, the materials consist of the photoconductive and second-order nonlinear optical moieties as the main components doped with small amount of sensitizer.<sup>7</sup> According to this principle, amorphous multifunctional chromophores combining both photoconductive and second-order nonlinear properties should be promising candidates. Suitable flexible alkyl chains introduced as plasticizers offer film-forming property and low glass–rubber transition temperature ( $T_g$ ). The  $T_g$  of photorefractive chromophores can be tuned by the use of different plastic chains.

In this paper, we report the synthesis and photorefractive properties of new carbazole conjugated trimers. In this approach, conjugated carbazole structure was used to design the photorefractive material system owing to excellent charge transporting properties and relatively high photogenerated carrier mobility of the conjugated carbazole polymers and oligomers.<sup>30</sup> It is generally assumed that materials with high charge carrier mobility are required to increase the speed of

photorefractive response. In these trimers, three carbazole rings are linked to each other by the ethynyl groups and peripheral carbazoles substituted with an electron-withdrawing group which make materials be electrooptically active. To obtain amorphous carbazole trimers with a low  $T_g$ , three long aliphatic groups are introduced to such trimer in the 9-position of each carbazole moiety. These amorphous trimers can function as both photoconductivity and EO activity.

## Experimental Section

**Materials and Characterization.** 3,6-Diiodocarbazole (**1**) and 3-iodocarbazole (**5**) were synthesized by the reaction reported by Tucker.<sup>31</sup> *N,N*-Dimethylformamide (DMF) and 1,2-dichloroethane were dried over molecular sieves. All other solvents and chemicals were used as received. Nuclear magnetic resonance (NMR) spectra were recorded on JEOL JNM-EX270 FTNMR system spectrometer operating at 270 MHz. Infrared (IR) spectra were measured on Shimadzu FTIR-4100 infrared spectrometer. Absorption coefficient were recorded with Shimadzu UV-3100 spectrophotometer. Melting points and glass transition temperature were obtained on Perkin-Elmer DSC-7. Elemental analyses were measured by Analytical Laboratory of RIKEN.

**3,6-Diiodo-9-tetradecylcarbazole (2).** To a solution of 3,6-diiodocarbazole (**1**) (5 g, 11.9 mmol) and 1-bromotetradecane (5 g, 18.1 mmol) in DMF (20 mL) was added potassium carbonate (5 g). After 12 h of stirring at ambient temperature, water (200 mL) was added to reaction mixture. The mixture was extracted with  $\text{CH}_2\text{Cl}_2$ , the organic phase was washed with water, dried over  $\text{Na}_2\text{SO}_4$ , and evaporated. The crude product was purified by column chromatography on silica gel using hexane as solvent; 7.0 g (96% yield) of 3,6-diiodo-9-tetradecylcarbazole (**2**) was obtained. Mp 73.5 °C.  $^1\text{H}$  NMR ( $\text{CDCl}_3$ , ppm): 8.27 (d, 2 H,  $J_1 = 1.65$  Hz), 7.67 (dd, 2 H,  $J_1 = 1.65$  Hz,  $J_2 = 8.85$  Hz), 7.13 (d, 2 H,  $J_2 = 8.58$  Hz), 4.17 (t, 2 H), 1.76 (m, 2 H), 1.20 (m, 22 H), 0.84 (t, 3 H). Anal. Calcd for  $\text{C}_{26}\text{H}_{35}\text{I}_2\text{N}$ : C, 50.75; H, 5.73; N, 2.28; I, 41.24. Found: C, 50.48; H, 5.68; N, 2.22; I, 41.45.

**3,6-Bis(trimethylsilyl)ethynyl-9-tetradecylcarbazole (3).** To a solution of 3,6-diiodo-9-tetradecylcarbazole (**2**) (5 g, 8.1 mmol) and trimethylsilylacetylene (2 g, 20 mmol) in triethylamine (30 mL) were added Pd( $\text{PPh}_3$ ) $_2\text{Cl}_2$  (100 mg) and CuI (50 mg). The reaction mixture was stirred at ambient temperature for 5 h under a slow stream of nitrogen. The reaction mixture was filtered. The residues were carefully washed with THF and the solvent evaporated from the combined filtrates. The crude product was purified by column chromatography on silica gel using hexane/ethyl acetate (9.5:0.5) as an eluent; 4.2 g (93% yield) of 3,6-di[(trimethylsilyl)ethynyl]-9-tetradecylcarbazole (**3**) as a viscous liquid was obtained.  $^1\text{H}$  NMR ( $\text{CDCl}_3$ , ppm): 8.19 (d, 2 H,  $J_1 = 1.32$  Hz), 7.58 (dd, 2 H,  $J_1 = 1.32$  Hz,  $J_2 = 8.25$  Hz), 7.28 (d, 2 H,  $J_2 = 8.25$  Hz), 4.24 (t, 2 H), 1.83 (m, 2 H), 1.23 (m, 22 H), 0.87 (t, 3 H), 0.28 (s, 18 H). IR (KBr): 2957, 2152, 1630, 1599, 1481, 1456, 1380, 1350, 1286, 1250, 1148, 933, 841, 806  $\text{cm}^{-1}$ .

**3,6-Diethynyl-9-tetradecylcarbazole (4).** To a solution of 3,6-di[(trimethylsilyl)ethynyl]-9-tetradecylcarbazole (**3**) (4 g, 7.2 mmol) in THF/MeOH (3:1) (50 mL) was added sodium hydroxide (1 g) in water (5 mL). The reaction mixture was stirred for 3 h at ambient temperature. Water (150 mL) was then added to the reaction mixture. The mixture was extracted with  $\text{CH}_2\text{Cl}_2$ , and the organic phase was washed with water and dried over  $\text{Na}_2\text{SO}_4$ . After the solvents were removed by evaporation, the crude product was purified by column chromatography on silica gel using hexane as solvent. 2.8 g (95% yield) of 3,6-diethynyl-9-tetradecylcarbazole (**4**) was obtained. Mp 28.9 °C.  $^1\text{H}$  NMR ( $\text{CDCl}_3$ , ppm): 8.21 (d, 2 H,  $J_1 = 1.32$  Hz), 7.60 (dd, 2 H,  $J_1 = 1.32$  Hz,  $J_2 = 8.25$  Hz), 7.32 (d, 2 H,  $J_2 = 8.25$  Hz), 4.26 (t, 2 H), 3.08 (s, 2 H), 1.87 (m, 2 H), 1.23 (m, 22 H), 0.88 (t, 3 H). IR (KBr): 3314, 2930, 2104,

(18) Tamura, K.; Padias, A. B.; Hall, Jr. H. K.; Peyghambarian, N. *Appl. Phys. Lett.* **1992**, *60*, 1803.

(19) Peng, Z.; Gharavi, A.; Yu, L. *Appl. Phys. Lett.* **1996**, *69*, 4002.

(20) Yu, L. P.; Chan, W. K.; Bao, Z. N.; Cao, S. X. *J. Chem. Soc., Chem. Commun.* **1992**, 1735.

(21) Zhao, C.; Park, C. K.; Prasad, P. N.; Zhang, Y.; Ghosal, S.; Burzynski, R. *Chem. Mater.* **1995**, *7*, 1237.

(22) Kawakami, T.; Sonoda, N. *Appl. Phys. Lett.* **1993**, *62*, 2167.

(23) Meerholz, K.; Volodin, B. L.; Sandalphone; Kippelen, B.; Peyghambarian, N. *Nature* **1994**, *371*, 497.

(24) Gunnet-Jepsen, A.; Thompson, C. L.; Twieg, R. J.; Moerner, W. E. *Appl. Phys. Lett.* **1997**, *70*, 1515.

(25) Lundquist, P. M.; Wortmann, R.; Geletneky, C.; Twieg, R. J.; Jurich, M.; Lee, V. Y.; Moylan, C. R.; Burland, D. M. *Science* **1996**, *274*, 1182.

(26) Zhang, Y. D.; Wada, T.; Wang, L.; Aoyama, T.; Sasabe, H. *Chem. Commun.* **1996**, 2325.

(27) Kippelen, B.; Tamura, K.; Peyghambarian, N.; Padias, A. B.; Hall, Jr., H. K. *Phys. Rev. B* **1993**, *48*, 10710.

(28) Wang, L.; Zhang, Y. D.; Wada, T.; Sasabe, H. *Appl. Phys. Lett.* **1996**, *69*, 728.

(29) Wada, T.; Wang, L.; Zhang, Y. D.; Tian, T.; Sasabe, H. *Nonlinear Optics* **1996**, *15*, 103.

(30) Beginn, C.; Grazulevicius, J. V.; Strohrriegel, P. *Macromol. Chem. Phys.* **1994**, *195*, 2353.

(31) Tucker, S. H. *J. Chem. Soc.* **1926**, 546.

1630, 1599, 1481, 1383, 1352, 1288, 1234, 1151, 885, 806  $\text{cm}^{-1}$ . Anal. Calcd for  $\text{C}_{30}\text{H}_{37}\text{N}$ : C, 87.59; H, 9.00; N, 3.41. Found: C, 87.74; H, 9.19; N, 3.36.

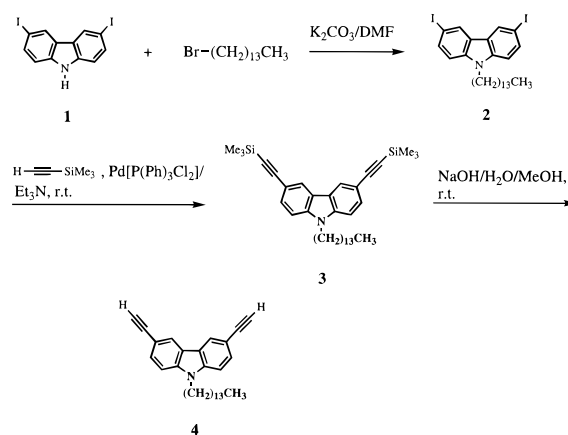
**3-Iodo-9-tetradecylcarbazole (6).** To a solution of 3-iodocarbazole (**5**) (5 g, 17.1 mmol) and 1-bromotetradecane (7 g, 25.3 mmol) in DMF (45 mL) was added potassium carbonate (8 g). After 12 h of stirring at ambient temperature, water (200 mL) was added to reaction mixture. The mixture was extracted with  $\text{CH}_2\text{Cl}_2$ , and the organic phase was washed with water, dried over  $\text{Na}_2\text{SO}_4$ , and evaporated. The crude product was purified by column chromatography on silica gel using hexane as solvent; 7.6 g (91% yield) of 3-iodo-9-tetradecylcarbazole (**6**) as a white solid was obtained.  $^1\text{H}$  NMR ( $\text{CDCl}_3$ , ppm): 8.38 (d, 1 H), 8.03 (d, 1 H), 7.63 (dd, 1 H), 7.41 (m, 2 H), 7.18 (m, 2 H), 4.25 (t, 2 H), 1.81 (m, 2 H), 1.22 (m, 22 H), 0.88 (t, 3 H).

**3-Iodo-6-formyl-9-tetradecylcarbazole (7).** To DMF (2 g, 0.027 mol) at 0  $^\circ\text{C}$ , phosphorus oxychloride (4.3 g, 0.028 mol) was added dropwise. After addition of phosphorus oxychloride, the reaction mixture was allowed to warm to room temperature, and 3-iodo-9-tetradecylcarbazole (**6**) (7 g, 0.014 mol) dissolved in 1,2-dichloroethane (20 mL) was added. Then the reaction mixture was heated to 90  $^\circ\text{C}$ . After the reaction was carried out at this temperature for 16 h, the reaction mixture was added to ice water (500 mL). The mixture was extracted with  $\text{CH}_2\text{Cl}_2$ , and the organic phase was washed with water, dried over  $\text{Na}_2\text{SO}_4$ , and evaporated. The crude product was purified by column chromatography on silica gel using hexane and ethyl acetate (7:3) as solvent; 5 g (69.4% yield) of 3-iodo-6-formyl-9-tetradecylcarbazole (**7**) as a white crystal was obtained. Mp 101.9  $^\circ\text{C}$ .  $^1\text{H}$  NMR ( $\text{CDCl}_3$ , ppm): 10.08 (s, 1 H), 8.53 (d, 1 H,  $J_1 = 1.65$  Hz), 8.44 (d, 1 H,  $J_2 = 1.65$  Hz), 8.04 (dd, 1 H,  $J_1 = 1.65$  Hz,  $J_3 = 8.58$  Hz), 7.78 (dd, 1 H,  $J_2 = 1.65$  Hz,  $J_4 = 8.58$  Hz), 7.47 (d, 1 H,  $J_3 = 8.58$  Hz), 7.23 (d, 1 H,  $J_4 = 8.58$  Hz), 4.29 (t, 2 H), 1.88 (m, 2 H), 1.22 (m, 22 H), 0.87 (t, 3 H). IR (KBr): 3273, 2930, 1628, 1593, 1514, 1475, 1329, 1296, 1230, 1149, 1093, 1018, 806  $\text{cm}^{-1}$ . Anal. Calcd for  $\text{C}_{27}\text{H}_{36}\text{INO}$ : C, 62.67; H, 6.96; N, 2.71; I, 24.56. Found: C, 62.54; H, 6.92; N, 2.83, I, 24.27.

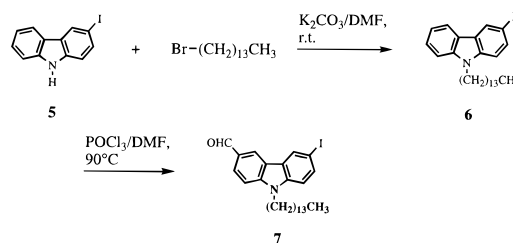
**3,6-Bis[(9-tetradecyl-6-formyl-3-carbazolyl)ethynyl]-9-tetradecylcarbazole (8).** To a solution of 3,6-diethynyl-9-tetradecylcarbazole (0.84 g, 2.04 mmol) and 3-iodo-6-formyl-9-tetradecylcarbazole (2.2 g, 4.26 mmol) in triethylamine (50 mL) were added  $\text{Pd}(\text{PPh}_3)_2\text{Cl}_2$  (40 mg) and  $\text{CuI}$  (20 mg). The reaction mixture was stirred at ambient temperature for 12 h under a slow stream of nitrogen. The reaction mixture was filtered. The residues were carefully washed with THF and the solvent was evaporated from the combined filtrates. The crude product was purified by column chromatography on silica gel using chloroform as an eluent; 1.84 g (77% yield) of 3,6-bis[(9-tetradecyl-6-formyl-3-carbazolyl)ethynyl]-9-tetradecylcarbazole (**8**) as a viscous liquid were obtained.  $^1\text{H}$  NMR ( $\text{CDCl}_3$ , ppm): 10.11 (s, 2 H), 8.60 (d, 2 H), 8.36 (dd, 4 H), 8.04 (dd, 2 H), 7.72 (m, 4 H), 7.44 (m, 6 H), 4.32 (m, 6 H), 1.88 (m, 6 H), 1.23 (m, 66 H), 0.87 (t, 9 H).

**3,6-Bis[(9-tetradecyl-6-dicyanovinyl-3-carbazolyl)ethynyl]-9-tetradecylcarbazole (10a).** To a solution of 3,6-bis[(9-tetradecyl-6-formyl-3-carbazolyl)ethynyl]-9-tetradecylcarbazole (**8**) (1.6 g, 1.3 mmol) and malononitrile (**9a**) (0.4 g, 6.1 mmol) in THF (30 mL) was added 4-(dimethylamino)pyridine (DMAP) (0.3 g). After the reaction mixture was stirred at ambient temperature in THF for 1 h, THF was removed, and the condensation reaction was then carried out in solid state for another 3 h. Water (100 mL) was added to reaction mixture. The mixture was extracted with  $\text{CH}_2\text{Cl}_2$ , and the organic phase was washed with water, dried over  $\text{Na}_2\text{SO}_4$ , and evaporated. The crude product was purified by column chromatography on silica gel using  $\text{CH}_2\text{Cl}_2$ /hexane (8:2) as an eluent. 1.4 g (83% yield) of 3,6-bis[(9-tetradecyl-6-dicyanovinyl-3-carbazolyl)ethynyl]-9-tetradecylcarbazole as a red glass solid was obtained.  $^1\text{H}$  NMR ( $\text{CDCl}_3$ , ppm): 8.65 (d, 2 H), 8.33 (dd, 4 H), 8.06 (dd, 2 H), 7.85 (s, 2 H), 7.77 (m, 4 H), 7.42 (m, 6 H), 4.32 (m, 6 H), 1.90 (m, 6 H), 1.24 (m, 66 H), 0.87 (t, 9 H). IR (KBr): 2924, 2222, 1562, 1493, 1390, 1351, 1234, 1151, 806  $\text{cm}^{-1}$ . Anal. Calcd for  $\text{C}_{90}\text{H}_{107}\text{N}_7$ : C, 84.00; H, 8.38; N, 7.62. Found: C, 83.82; H, 8.43; N, 7.36.

### Scheme 1



### Scheme 2

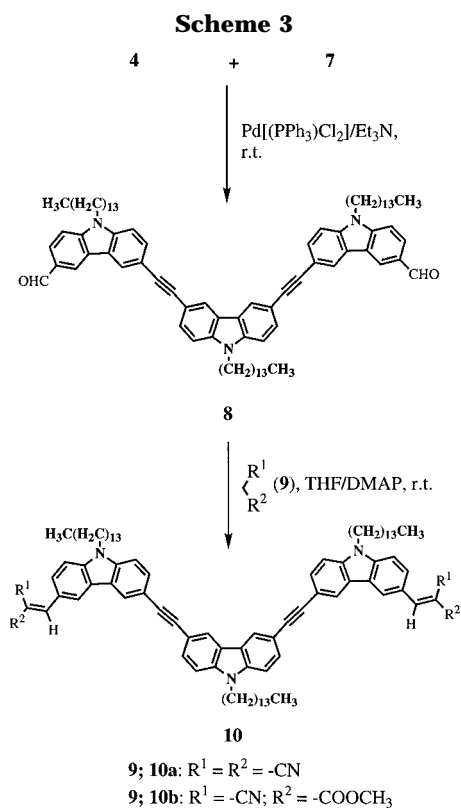


**3,6-Bis[(9-tetradecyl-6-cyanoacetoxyvinyl-3-carbazolyl)ethynyl]-9-tetradecylcarbazole (10b).** To a solution of 3,6-bis[(9-tetradecyl-6-formyl-3-carbazolyl)ethynyl]-9-tetradecylcarbazole (**8**) (0.5, 0.42 mmol) and cyanoacetic acid methyl ester (**9b**) (0.4 g, 4.0 mmol) in THF (30 mL) was added DMAP (0.2 g). After the reaction mixture was stirred at ambient temperature in THF for 1 h, THF was removed, and the condensation reaction was then carried out in solid state for another 3 h. Water (30 mL) was added to reaction mixture. The mixture was extracted with  $\text{CH}_2\text{Cl}_2$ , and the organic phase was washed with water, dried over  $\text{Na}_2\text{SO}_4$ , and evaporated. The crude product was purified by column chromatography on silica gel using  $\text{CH}_2\text{Cl}_2$ /hexane (8:2) as an eluent. 0.5 g (87% yield) of 3,6-bis[(9-tetradecyl-6-cyanoacetoxyvinyl-3-carbazolyl)ethynyl]-9-tetradecylcarbazole as a glass yellow solid was obtained.  $^1\text{H}$  NMR ( $\text{CDCl}_3$ , ppm): 8.77 (d, 2 H), 8.43 (s, 2 H), 8.38 (dd, 4 H), 8.23 (dd, 2 H), 7.81 (m, 4 H), 7.41 (m, 6 H), 4.33 (m, 6 H), 3.95 (s, 6 H), 1.90 (m, 6 H), 1.23 (m, 22 H), 0.87 (m, 9 H). IR (KBr): 2924, 2218, 1726, 1628, 1581, 1493, 1466, 1390, 1354, 1282, 1259, 1228, 1182, 1159, 1134, 1093, 881, 806  $\text{cm}^{-1}$ . Anal. Calcd for  $\text{C}_{92}\text{H}_{113}\text{N}_5\text{O}_4$ : C, 81.67; H, 8.42; N, 4.94. Found: C, 81.22; H, 8.38; N, 4.94.

**Film Preparation.** Carbazole trimer **10a** and different mole percents of 2,4,7-trinitro-9-fluorenone (TNF) were dissolved in dichloromethane. After removal of solvent, samples of carbazole trimer containing 0.20, 0.24, 0.25, 0.51, and 2.01 mol % of TNF were obtained and sandwiched between two indium tin oxide (ITO) covered glass substrates for photorefractive measurements or the Al-covered glass substrate and ITO-covered substrate for photoconductive measurements. Films could be obtained at 60  $^\circ\text{C}$  at which the carbazole trimer **10a** doped with TNF melted. Thickness of films could be guaranteed by a Teflon film spacer. This Teflon film spacer was also acted as insulator to resist the high voltage between the two electrodes.

## Results and Discussion

**Synthesis.** The synthetic procedure is shown in Schemes 1–3. 3,6-Diiodocarbazole (**1**) and 3-iodocarbazole (**5**) were obtained according to the method reported.<sup>27</sup> 3,6-Diiodo-9-tetradecylcarbazole (**2**) and 3-iodo-9-tetradecylcarbazole (**6**) were synthesized by



nucleophilic substitution reaction of 1-bromotetradecane with 3,6-diiodocarbazole (**1**) and 3-iodocarbazole (**6**), respectively. 3,6-Diethynyl-9-tetradecylcarbazole (**4**) was prepared from 3,6-diiodo-9-tetradecylcarbazole and trimethylsilylacetylene by Pd-catalytic coupling reaction and followed by the removal of trimethylsilyl group from 3,6-di(trimethylsilylethynyl)-9-tetradecylcarbazole (**3**). 3-Iodo-6-formyl-9-tetradecylcarbazole (**7**) was yielded by the treatment of 3-iodo-9-tetradecylcarbazole with DMF/POCl<sub>3</sub>. Carbazole trimer (**8**) with two formyl groups could be synthesized from **4** and **7** by Pd-catalytic coupling reaction. Carbazole trimer **10** substituted with acceptor groups could be obtained by Knoevenagel condensation of **8** and **9** using DMAP as a base.

Differential scanning calorimetric (DSC) analysis shown in Figure 1 exhibited only glass transition for the trimers **10a** and **10b**. The  $T_g$  of trimers **10a** and **10b** were found to be 30 and 27 °C, respectively. The low  $T_g$  of these two trimers are due to three long plastic alkyl chains attached on each trimers. Other phase transitions, such as crystalline and recrystallization, at certain temperature range from 10 to 160 °C could not be observed from the trimers by DSC with the heating rate of 10 °C/min. The glassy states of the carbazole trimer **10a** and **10b** were also confirmed by a X-ray diffraction (XRD). It is well-known that the crystalline samples exhibit the XRD patterns with the sharp peaks. However, the carbazole trimers **10a** and **10b** show the XRD patterns with the broad halos (Figure 2). These morphological characteristics suggest that the trimers are fully amorphous.

Recently, bifunctional chromophores have been developed for photorefractive materials.<sup>16,17</sup> However, these chromophores should be used as a dopant dispersed into polymer matrix for photorefractive applications due to their crystalline nature. Amorphous chromophores with both charge transporting and electrooptic

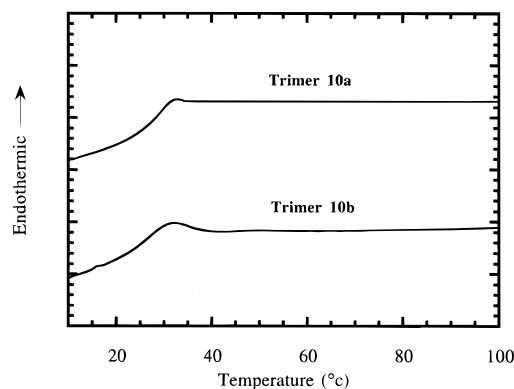


**Figure 1.** DSC thermograms of the carbazole trimers at 10 °C/min.

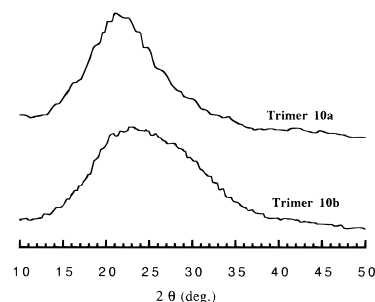


**Figure 2.** XRD pattern of the carbazole trimers.

functions have also been reported by two research groups.<sup>25,32</sup> Many of them were mixed with other amorphous polymers and/or the plasticizers in order to obtain long-time stable films. In our case, long-time stable films could directly be obtained from these carbazole trimer chromophores without supporting matrix and plasticizers due to both their fully amorphous state and their suitable  $T_g$ . Films of the trimers were found to be very stable and show no tendency to crystallize even after 2 years at room temperature.

The UV-visible spectrum of carbazole trimer **10a** shows absorption maximum at 412 nm in dioxane solution. Films of **10a** do not exhibit any absorption coefficient at the operating laser wavelength of 633 nm. At this wavelength, photocharge generation cannot be achieved in pure carbazole trimer **10a**. However, photocharge generation efficiency can be enhanced by the formation of the charge-transfer (CT) complex between carbazole unit and TNF. The absorption tail of carbazole trimer doped with TNF appears at the long wavelength due to the formation of CT complex of carbazole moiety with TNF. The resulting CT complex could generally be characterized by an absorption band in the visible or near-infrared, which does not appear in the pure TNF or pure carbazole trimer **10a**. It was found that the absorption coefficient of **10a** doped with TNF at a wavelength of 633 nm increased with the mole percent of TNF. Figure 3 shows the absorption coefficient at 633 nm as a function of the mole percent of TNF. This absorption coefficient due to the formation of CT complex could extend the photoconductive activity of the trimer to a longer wavelength of 633 nm. Illumination of the doped trimer with a wavelength of 633 nm should induce photocarrier generation due to the CT transition in this photorefractive trimer.

(32) Bolink, H. J.; Arts, C.; Krasnikov, V. V.; Malliaras, G. G.; Hadjioannou, G. *SPIE* **1996**, *2850*, 69.

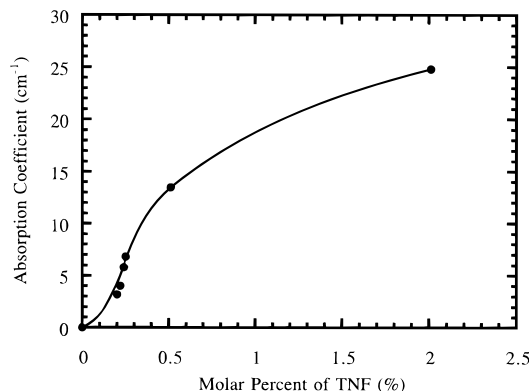


**Figure 3.** Absorption coefficient of the carbazole trimer **10a** at a wavelength of 633 nm as a function of the mole percent of TNF.

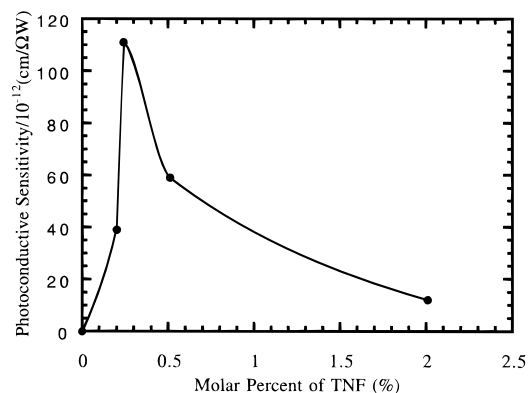


**Figure 4.** Photoconductive sensitivity of the carbazole trimer **10a** as a function of the mole percent of TNF at an applied electric field of 30.7 V/μm.

The photoconductive measurements were performed on about 10.5 μm thick samples sandwiched between Al and ITO electrodes at a wavelength of 633 nm using a photocurrent method.<sup>33</sup> The photoconductive sensitivity ( $S$ ) could be calculated from the experimentally measured photocurrent ( $I_{ph}$ ) according to eq 1, where  $L$

$$S = (I_{ph}L)/AVI_0 \quad (1)$$

is the sample thickness,  $A$  is the illumination area,  $V$  is the applied dc voltage, and  $I_0$  is the illumination laser power density. Concentration of TNF has a significant influence on photoconductive sensitivity. Photocurrent could not be observed from pure trimer sample at a wavelength of 633 nm. However, the trimer doped with TNF exhibited photocurrent under a driven electric field. A maximum value of photoconductive sensitivity was observed in a 0.24 mol % TNF doped sample. Figure 4 displays the photoconductive sensitivity as a function of the mole percents of TNF at an applied electric field of 30.7 V/μm. Photoconductivity is influenced by two processes: charge generation and charge transporting. The charge generation efficiency increased with the TNF doping concentration due to the increase of the CT complex density. However, the free TNF as a trap for holes increased simultaneously. The density of uncomplexed central carbazole of the trimer **10a** as a hole transporting moiety decreased and sensitively influenced the magnitude of drift mobility.

(33) Schildkraut, J. S. *Appl. Phys. Lett.* **1991**, *58*, 340.

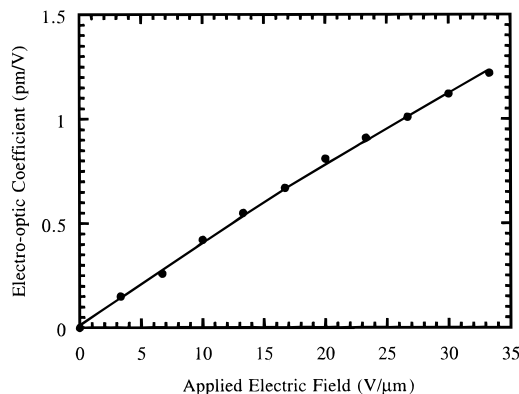


**Figure 5.** Electrooptic coefficient of the carbazole trimer **10a** doped with 0.024 mol % of TNF as a function of the applied electric field.

There is, therefore, a balance between the charge generation and charge transporting processes, which results in observation of an optimization of TNF concentration in the trimer photoconductivity.<sup>34</sup> Photoconductivity is one of the main function, for photorefractive materials. Detailed research work on relationship between the photoconductivity and the TNF concentration is now underway. The carbazole trimer **10a** doped with 0.24 mol % of TNF was used as an example for measurements of the electrooptic properties and photorefractive effects in this work. The refractive index of 1.687 at a wavelength of 633 nm was determined from a 2 μm thick spin-coating film on fused silica glass slides by mode line measurement.<sup>35</sup>

Due to the low  $T_g$  of the trimer, the chromophores could be effectively aligned at room temperature by an applied dc electric field across the sample. The EO coefficient was measured on the same sample as that for the photorefractive measurements using transmission technique.<sup>36</sup> In the general case, at low ac frequencies, large EO effect could be observed due to the contributions from both the field induced birefringence and the EO effect.<sup>37,38</sup> More accurate measurements of EO coefficients should be performed at high modulation ac frequencies at which the birefringence effect is insignificant and only the EO effect of chromophores can respond to the applied ac frequencies.<sup>37</sup> To avoid the contribution from birefringence (molecular orientation), the EO coefficients of the trimer **10a** were measured at a relatively high modulation ac frequency (6 kHz). Figure 5 shows the electric field dependence of the EO coefficient without contribution from birefringence. These value are comparable with those obtained from other photorefractive material systems.<sup>7,38</sup>

The photorefractive properties of carbazole trimer **10a** containing 0.24 mol % of TNF with 130 μm thick film were studied by the two-beam coupling and four-wave mixing. In the two-beam coupling experiment, holographic gratings were written by two p-polarized laser beams at a wavelength of 633 nm from a He-Ne laser. Two writing beams with an equal intensity of 250 mW/

(34) Gill, W. D. *J. Appl. Phys.* **1972**, *43*, 5033.

(35) Tien, P. K.; Ulrich, R.; Marti, R. J. *Appl. Phys. Lett.* **1969**, *14*, 291.

(36) Teng, C. C.; Man, H. T. *Appl. Phys. Lett.* **1990**, *56*, 1735.

(37) Moerner, W. E.; Silence, S. M.; Hache, F.; Bjorklund, G. C. J. *Opt. Soc. Am. B* **1994**, *11*, 320.

(38) Cox, A. M.; Blackburn, R. D.; West, D. P.; King, T. A.; Wade, F. A.; D. A. Leigh, D. A. *Appl. Phys. Lett.* **1996**, *68*, 2801.

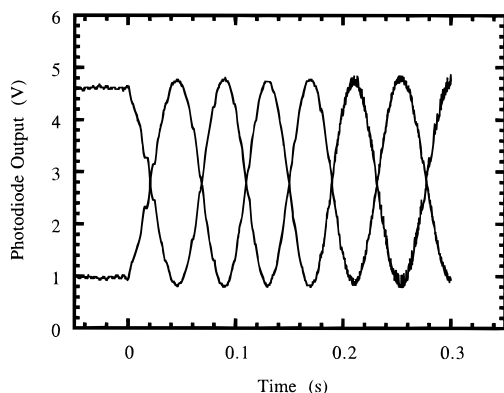


**Figure 6.** Transmitted intensities of the two coupling beams at an applied electric field of 27.8 V/ $\mu\text{m}$  when the sample was translated at  $t = 0.0$  s with a speed of 48  $\mu\text{m}/\text{s}$  and stopped at  $t = 0.3$  s.

$\text{cm}^2$  intersect in the sample. The normal of the sample surface was tilted  $60^\circ$  to yield a projection of the grating wave vector along the poling axis. With this geometry, an intensity grating period of around 3.9  $\mu\text{m}$  was created.

To unambiguously distinguish nature between the space charge field induced photorefractive effect and other types of gratings, a two-beam coupling measurement must be performed. The refractive index grating can be obtained from the existence of a spatial phase shift between the illumination pattern and the refractive index grating by a two-beam coupling experiment. According to the standard model of photorefractivity,<sup>39</sup> this phase shift increased with the applied electric field. At low electric fields, the phase shift is a nonzero between 0 and  $90^\circ$ . At relative high fields, the phase shift approaches  $90^\circ$ . To measure the phase shift of index grating, the sample was translated 14.4  $\mu\text{m}$  within 0.3 s in the direction of the grating wave vector by a piezoelectric stage (Physik Instrumente, P-841.10) after the stable grating was formed.<sup>40</sup> The transmitted signals of the two beams were detected with two large-area photodiodes (Hamamatsu Photonics, S2386) and recorded by a digital oscilloscope (LeCroy 9310). From the two-beam coupling experiment, the phase shift could be obtained from recorded transmitted intensities of the two beams. It was found that the phase shift of our trimer **10a** doped with 0.24 mol % of TNF increased with the applied electric field and achieved at  $90^\circ$  at an electric field above 20 V/ $\mu\text{m}$ . A typical recorded transmitted intensities of the two beams at an applied electric field of 27.8 V/ $\mu\text{m}$  is shown in Figure 6. The phase shift of about  $90^\circ$  could be deduced from the pattern of transmitted intensities of two beams. This result suggests that a clearly nonlocal photorefractive nature has been obtained from this low  $T_g$  carbazole trimer **10a** doped with 0.24 mol % of TNF.

An important consequence of the phase shift is an energy transfer between the two beams interfering in a photorefractive medium. This is also a unique effect which does not occur in any of the other processes which might result in refractive index gratings. Therefore, the photorefractive nature can be further confirmed by observation of the asymmetric energy transfer in two-

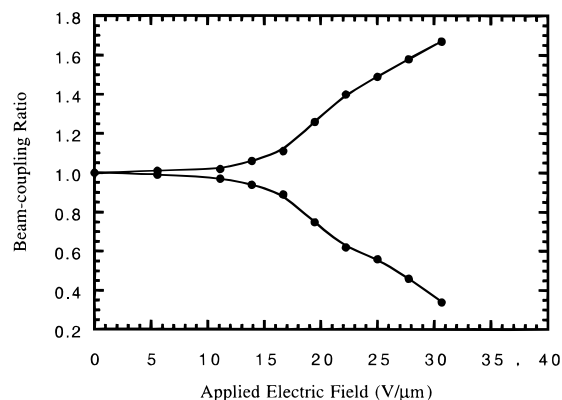


**Figure 7.** Beam-coupling ratio of the carbazole trimer **10a** doped with 0.24 mol % of TNF versus applied electric field.

beam coupling experiments. An asymmetric energy transfer between the two beams was observed in the trimer **10a** doped with TNF by monitoring the intensity of each of the two writing beams, when the applied electric field was switched on. The beam 1 coupling ratio ( $I_1/I_{1(t=0)}$ ) could be obtained from asymmetric energy transfer.  $I_{1(t=0)}$  is the intensity of beam 1 through the sample without beam 2, and  $I_1$  is the intensity of beam 1 through the sample with beam 2. Correspondingly, the beam 2 coupling ratio ( $I_2/I_{2(t=0)}$ ) could also be obtained from the asymmetric energy transfer and is complemented by an approximated equal decrease.  $I_{2(t=0)}$  is the intensity of beam 2 through the sample without beam 1, and  $I_2$  is the intensity of beam 2 with the beam 1. Figure 7 shows that the beam coupling ratio between the two beams as a function of the applied electric field. At an applied electric field of 30.7 V/ $\mu\text{m}$ , the beam coupling ratio was obtained as 1.67 and 0.34 for beam 1 and beam 2, respectively. Thus, the data are in good agreement, indicating that the beam 1 gained 67% of its intensity from the beam 2, at the same time the beam 2 lost 66% of its intensity.

Using two writing beams with equal powers ( $P_{\text{beam1}}/P_{\text{beam2}} = 1$ ), the photorefractive net gain ( $\Gamma_{\text{net}}$ ) could be determined from the beam coupling ratio by eq 2:<sup>41</sup>

$$\Gamma_{\text{net}} = (1/L)[\ln(\gamma_0) - \ln(2 - \gamma_0)] - \alpha \quad (2)$$

where  $L$  is the optical path length through the sample and  $\gamma_0$  is the beam coupling ratio between the two writing beams. The photorefractive two-beam coupling net gain increased with the applied electric field and reached 76  $\text{cm}^{-1}$  at an applied electric field of 30.7 V/ $\mu\text{m}$ . It is worth pointing out that the majority of applications for photorefractive materials require net gain. Our trimer exhibit a large net two-beam coupling gain since the gain greatly surpasses the absorption coefficient of 5.8  $\text{cm}^{-1}$  at the operation wavelength (633 nm). This result suggests that the molecular design for photorefractive materials based on conjugated carbazole oligomer system should be reasonable.

Four-wave mixing experiment was carried out with two s-polarized writing beams ( $2 \times 196 \text{ mW}/\text{cm}^2$ ) and a weak (14  $\text{mW}/\text{cm}^2$ ) p-polarized reading beam. The reading beam propagated in the direction opposite to one of the writing beams and was diffracted in the direction opposite to that of other writing beam. A

(39) Jones, B. E.; Ducharme, S.; Liphardt, M.; Goonesekera, A.; Takacs, J. M.; Zhang, L.; Athalye, R. *J. Opt. Soc. Am. B* **1994**, *11*, 1064.  
(40) Sutter, K.; Günter, P. *J. Opt. Soc. Am. B* **1990**, *7*, 2274.

(41) Hiugnard, J. P.; MARRAKCHI, A. *Opt. Commun.* **1981**, *38*, 249.

polarizing beam splitter was used to separate diffracted light. The diffracted light was detected by a photodiode. It was found that the diffraction efficiency strongly depended on the applied electric field and reaches 18.3% at an electric field of 30.6 V/ $\mu\text{m}$ . This field dependence is the typical nature of low  $T_g$  materials since the EO coefficient and the photorefractive properties are both electric field dependent.

In conclusion, amorphous conjugated carbazole trimers have been developed for photorefractive materials. The trimer substituted with dicyanovinyl group sensitized with TNF exhibited large photorefractive net gain and high diffraction efficiency. It was found all photorefractive properties were strongly dependent on the

applied electric field and mole percent of TNF. The study of the photorefractive behaviors at a high electric field and the dynamic of the grating formation and photoconductivity is now in progress. It should be pointed out that photorefractive optical gain and diffraction efficiency might be contributed from both EO and birefringence mechanisms due to the low  $T_g$  nature of the trimer.

**Supporting Information Available:** UV-vis spectra of pure trimer and trimer doped with TNF (1 page). Ordering information is given on any current masthead page.

CM970127W